



African Journal of Biological Sciences



Fabrication And Evaluation Of Chitosan–Based Electrospun Nanofibers Loaded With Environmentally Synthesized Silver Nanoparticles For Enhanced Wound Healing

Aarti Puri¹, Tanzeel Ahmed^{1*}, Nitin Sahai²

¹*School of Biotechnology, IFTM University, Delhi Road, NH-24 Moradabad, Lodhipur Rajput, Uttar Pradesh 244102, India, aartipuri1958@gmail.com, tanzeel_ahmad@iftmuniversity.ac.in*

²*Department of Biomedical Engineering, North Eastern Hill University, Shillong 793022, Meghalaya, India, nitinbiomedical@gmail.com*

***Corresponding Author:** Tanzeel Ahmed

**School of Biotechnology, IFTM University, Delhi Road, NH-24 Moradabad, Lodhipur Rajput, Uttar Pradesh 244102, India*

Volume 6, Issue 6, June 2024
Received: 06 April 2024
Accepted: 11 May 2024
Published: 07 June 2024
doi: 10.33472/AFJBS.6.6.2024.2382–2392

ABSTRACT

Scientists' fascination with using electrospinning to create dressings for wounds has grown in the last several years. The resulting pads of electrospun nanofibers feature exceptional qualities such as a high flexibility, porosity, surface-to-volume ratio, and the ability to suck fluid from injuries, in addition to the method's simplicity, adaptability, and scalability. This study aims to synthesize and characterize chitosan-based electrospun nanofibers that are rich in environmentally benign AgNPs. The environmentally friendly silver nanoparticles were created utilizing a green method involving plant extracts and electrospun from a chitosan solution. Using Fourier-transform infrared spectroscopy (FTIR), X-ray diffraction (XRD), scanning electron microscopy (SEM), and differential scanning calorimetry analysis (DSC), the resultant nanofibers were examined for their morphology, structure, and chemical makeup. The XRD and FTIR measurements verified the effective incorporation of silver nanoparticles into the chitosan nanofibers. Because the polymer mixture has a high tension on its surface, the CT + PEO + AgNP combination of electrospun nanofibers demonstrated excellent-quality fibers with an average fiber diameter of about 150 nm.

Keywords: *Electrospinning, Chitosan, green synthesized silver nano particle, PEO, Characterization, nanofibers.*

1. INTRODUCTION

Skin injuries are a serious healthcare issue that has elevated rates of death and disability. Despite the recent developments in wound dressing systems, the issue of the inadequate efficiency of available therapies persists (Mirhaj et al. 2022; Pourshahrestani et al. 2020). Antibiotic-resistant bacteria are spreading, making the use of antibiotics to prevent and treat wound infections futile (Tan et al. 2020). It also comes at an additional expense to the sufferer and society. Consequently, it is imperative to look into cutting-edge methods for developing fresh technologies that operate better at accelerating skin renewal and healing from wounds. Numerous experimental studies on a

variety of cells, including mesenchymal stem, bone and cartilage, neuron, and heart cells, have shown that electrical stimulation has an impact on the main behaviors of cells, including adherence, differentiation, proliferation, and motility (Vandghanooni and Eskandani 2019; Chen et al., 2019). The scientific community has become increasingly interested in using electrospinning to make wound dressings in recent years (Stoica et al. 2020; Shahid et al. 2021). The latest advanced methods like 3D bioprinting can be applied for diagnostic and therapeutic purposes (Puri *et al.* 2023). In addition to the method's ease of use, adaptability, and scalability, the produced electrospun nanofiber mats have exceptional qualities such as a high flexibility, high porosity, surface-to-volume ratio, and the ability to absorb wound exudate. These membranes' nanoscale characteristics allow them to imitate the composition of the extracellular matrix (ECM), which aids in the proliferation, adhesion, and migration of the cells and aids in the regeneration of damaged skin (Anjum et al. 2022). Furthermore, because nanofiber scaffolds have a large specific surface area and a lot of pores, these features make them a good substrate for cell adhesion. Furthermore, the tiny pore dimensions and tightly connected pore network allow for oxygen as well as water permeability in along with preventing microbial infiltration and the development of diseases. Its capacity to hold biologic substances that directly contribute to the recovery process while guaranteeing their continuous distribution to the area of injury is another sign of these membranes' fascinating capability to serve as advanced biologically responsive dressings. These characteristics all have a role in how well a wound heals. Electrospinning is a productive method that yields continuous nanofibers with typical sizes between a few tens and hundreds of nanometers, which are between 100 and 10,000 times smaller than fibers made by solution or melt spinning (Cui et al. 2021).

The prospective use of organic, biodegradable products in the creation of ecologically sound dressings for wounds has arisen from the wound care industry's strong desire for environmentally friendly alternatives. The natural biopolymer chitosan (CS), which is produced via chitin deacetylation, is found on the shells of crustaceans (including prawns, crabs, and lobsters), algae cell walls, fungi, etc. (Elsoud et al. 2022). Known for its excellent biocompatibility, non-toxicity, antibacterial action against a broad spectrum of pathogenic organisms, non-immunogenicity, and rapid biodegradability, this naturally occurring polysaccharide has generated significant attention in a variety of biological applications (Sahai *et al.* 2021). N-acetyl glucosamine, a monomer found in chitosan, is being shown to facilitate hemostasis, stimulate cell division, and hasten wound healing. Additionally, adding silver nanoparticles (AgNPs) to wound dressings has shown to have a remarkable potential for speeding up the healing process. AgNPs have special antibacterial qualities that enable them to be effective against a variety of diseases that can obstruct the healing process. AgNPs were created using eco-friendly processes, which is in line with the increased focus on eco- and sustainably produced materials in the field of nanomedicine. This work aims to synthesise and characterise chitosan electrospun nanofibers equipped with environmentally benign AgNPs. The resulting nanocomposite dressing is anticipated to provide a variety of benefits, including accelerated wound healing, tissue regeneration, and antibacterial activity. This work, which explores the potential of these innovative wound dressings for quicker and enhanced wound healing results, aims to close the gap between advanced nanotechnology and wound care in this setting. This inquiry seeks to provide insightful information into the design and development of next-generation wound dressings, providing creative solutions to the urgent problems of chronic wound treatment.

2. MATERIALS AND METHODS

2.1. Green synthesis of silver nanoparticles

Aloe vera, *Ocimum tenuiflorum* (Holy Basil), *Syzygium cumini* (Jamun), *Ficus carica* (Fig), and *Tridax procumbens* are among the medicinal plants whose leaves were gathered and whose extracts were made using a methanol solution. A common approach involved combining 5 mL of the leaf extract with 50 mL of a room-temperature aqueous solution containing 1×10^{-3} M AgNO_3 . The solution turned grey-black after 60 minutes, indicating that silver nanoparticles (AgNPs) had successfully formed.

2.2. Preparation of electrospinning solutions and electrospinning

Polyethylene oxide (PEO) and chitosan were formed into distinct formulations, each with a particular concentration: 8% (w/v) PEO and 3% (w/v) chitosan. These solutions underwent painstaking optimisation. They were then merged 50/50 and blended together using the sonication technique to produce a composite sample known as CT + PEO. A composite sample known as CT + PEO + AgNP was created by adding a 4-weight percent solution of silver nanoparticles (AgNP) made using green synthesis in a separate stage to the CT + PEO polymer solution. All samples were processed using a pump, and the needle's tip received a 15 kV power supply. The nanofibers were deposited onto a collector that was 15 cm away from the needle at a flow rate of 1 mL/h. The revolving collector was surrounded by an aluminium sheet that was coated with nanofibers and connected to a negative electrode by a wire. The spinning process took place at a relative humidity of 40%–60% and a temperature of 25°C. The flow of the solution was aided by gravity, while the spinning produced electrostatic forces. After whirling around any acetic acid that persisted could be effectively eliminated by using deionized water to wash the nanofiber matrix until the pH was neutral. The nanofibers were subsequently prepared for characterisation examination by being dried in a vacuum oven for 24 hours.

2.3. Characterization

2.3.1. SEM analysis

Utilizing scanning electron microscopy (SEM), the shape and structure of the nanoparticle surfaces was investigated. A drop of the nanoparticle dispersion was applied to the aluminium stubs that were discernible on the specimen stub's surface, and it was then let to dry. The Auto Fine Platinum Coater was then used to apply a platinum layer to the stub prior to imaging. The morphological structure and fiber diameter were investigated using a SEM with a 10 kV acceleration voltage. Preceding to the experiment, the samples were given a gold sputter coating in an argon atmosphere to make them electrically conductive. Porosity and fiber diameter were also calculated.

2.3.2. XRD Measurements

A STADI-P diffractometer, made by Stoe in Darmstadt, Germany, was used to gather data on X-ray powder diffraction for the sample CT + PEO + AgNP. The diffractometer used transmission-geometry-configured Ge (111) crystals to filter monochromatic $\text{Cu K}\alpha$ light with a wavelength of 1.54056Å. The X-ray source used 40 mA and 40 kV to operate. The samples were put between two acetate-cellulose foils in order to get them ready for analysis. A Mythen 1K detector made by Dectris in Baden, Switzerland, was used to capture the diffraction pattern. Data points were collected at intervals of 0.015° and covered the 2θ range between 3° and 61°. Over the course of 60 seconds, each data point was integrated at each 1.05° increment in the scanning range.

2.3.3. FTIR

Using the Fourier transform infrared spectra (ATR FTIR), the electrospun nanofibers' chemical group was determined (Perkin-Elmer, USA). Specimen granules were formed by cutting small portions of the sample nanofibers, combining them with KBr, and pressing them together. Readings were taken between 4000 and 400 cm^{-1} at a resolution of 2 cm^{-1} .

2.3.4. DSC analysis

On the basis of the endothermic process, thermal examination of nanofibrous materials was carried out using differential scanning calorimetry (METTLER TOLEDO, Switzerland). At an intensity of 10°C per minute, the test specimens were elevated from ambient temperature to 250 °C, and 50 mL of nitrogen were pumped through them every minute.

3. RESULT AND DISCUSSION

Maintaining wounds is essential, especially for diabetic patients and people who have suffered burns. The wound becomes a part of the skin after it has been created, and bacteria thrive there. Depending on the wound's location, kind, and management, the healing process can begin. Both external and internal factors have the potential to obstruct the healing process. Following the release of cytokines that cause cell migration and proliferation, the internal prerequisite step in wound healing occurs. Reactive oxygen species and bacterial infections are significant hindrances to the wound healing process that can delay each phase.

Fabricating chitosan into submicron-sized fibrous structures poses a significant challenge due to its inflexible sequences of D-glucosamine and its tendency to form intra- or inter molecular H bonds. This results in reduced dispersion in typical organic solvents as well as pure water. Chemical transformation is an alternate strategy to improve chitosan's solubility and spinnability, as demonstrated by Geng et al. in 2005. However, a more straightforward method for refining the spinnability of chitosan is by amalgamation it with another polymer, whether of synthetic or natural origin, such as PEO, or by incorporating green-synthesized nanoparticles, as suggested by Bösiger et al. in 2018. These advancements have given rise to a novel category of wound dressings composed of chitosan-based nanofibers. These wound dressings exhibit exceptional properties, including superior biocompatibility, biodegradability, porosity, and antimicrobial activity, as highlighted by the work of Antunes et al. in 2015.

3.1. SEM analysis

Significant morphological alterations in nanofibrous mats were seen in SEM pictures. The superficial morphology of the synthesised nanofibrous mats is shown in Figure 1, which demonstrates that every structure has nanoscale fibres similar to the structural network present in native tissue (Khodadoust et al., 2018). Owing to the polymer solution's elevated tension on its surface, the CT + PEO + AgNP combination among the electrospun nanofibers showed high-quality fibres with little bead formation. Ag NPs increased the electrospinnability of the polymer solution, producing non-beaded fibres that were more consistent and uniform. Ag NPs were added to the nanofiber surface, which enhanced the charge density and reduced the fibre diameter. The creation of a Taylor cone was induced by a spike in electric currents on the exterior of the polymer droplet at the point of injection due to enhanced conductivity. As a result, improved conductivity increased the polymer solution's ability to stretch and led to the electrospinning process' creation of fibres with smaller diameters (Angamma and Jayaram, 2011; Jirofti et al., 2021).

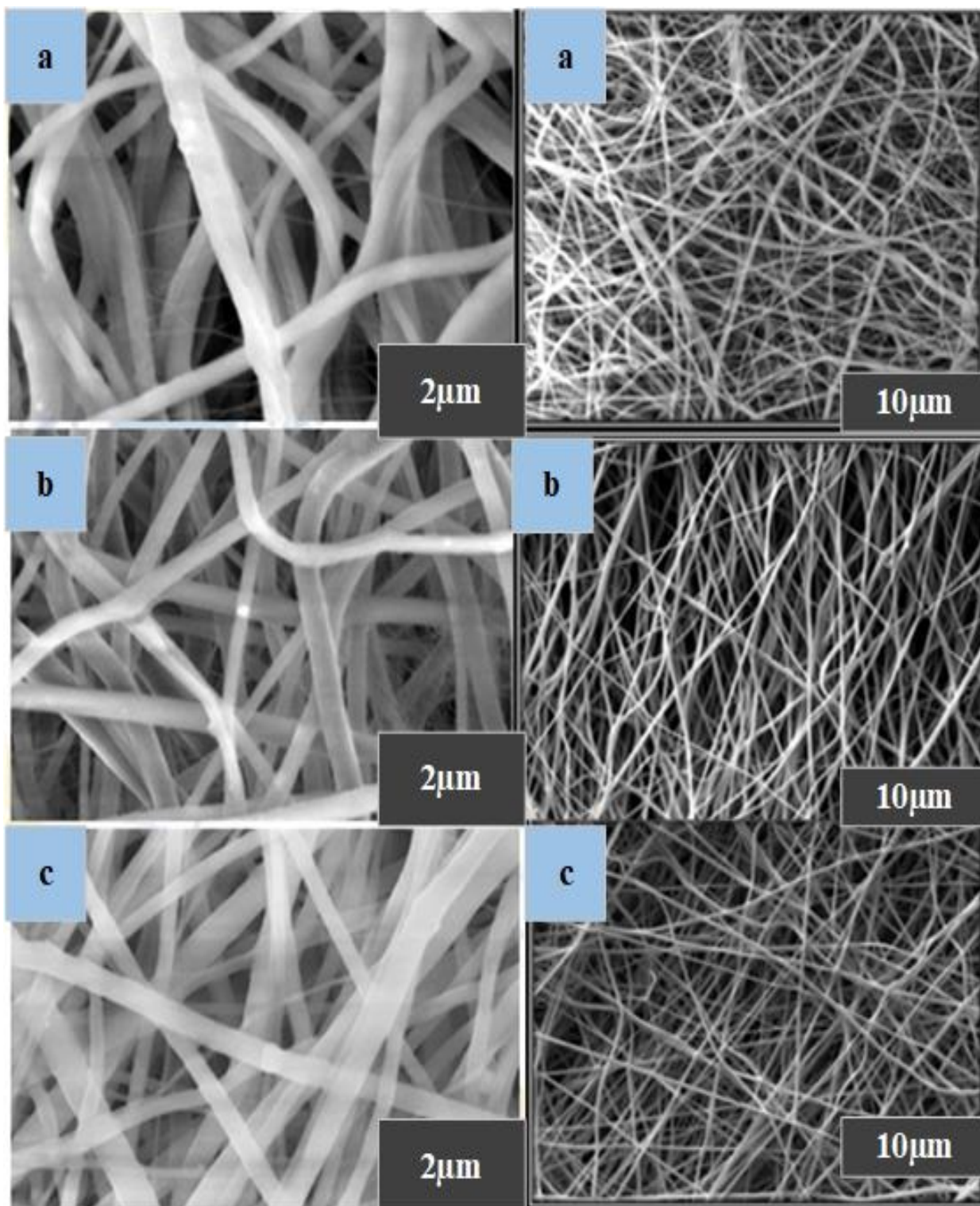


Figure 1: SEM images of the samples. (a) CT; (b) CT + PEO; and (c) CT + PEO + AgNP.

3.2. Fiber density and porosity measurement

Silver nanoparticles were added to the Chitosan PEO polymer solution to help the electrospinning process run smoothly and produce homogeneous, bead-free nanofibers with a size in the nanoscale range. For chitosan (CT) and chitosan with polyethylene oxide (CT + PEO), the average fibre sizes were determined at 92 nm and 132 nm, respectively. It is noteworthy that the addition of green-synthesized nanoparticles to the polymer solution caused a significant increase in fibre diameter, which increased to an average of 158 ± 25 nm and surpassed the dimensions of the control

nanofibers (Figure 2). With an ideal fibre diameter of 150 nm, this uniform and smooth form is particularly good at encasing silver nanoparticles for potential applications in the management of microbially-infected wound recovery. As formerly testified by Ganesh et al. in 2016 and Shi et al. in 2016, the unique characteristics of these nanofibers imply that the polymer scaffold and the silver nanoparticles have created linkages through bonds of hydrogen, inhibiting the expansion and uptake of water by the drug-loaded nanofibers.

Chitosan (CT) and Chitosan with Polyethylene Oxide (CT + PEO) nanofibers were reported to have mean porosities of 85 ± 0.39 and 82 ± 0.46 , respectively. The porosity, on the other hand, marginally dropped to 79 ± 0.58 in the case of the AgNP-loaded Chitosan with Polyethylene Oxide (CT + PEO) nanofibers (Figure 2). As stated in the work by Srivastava et al. in 2019, a mean porosity of 80% was found by porosity testing the Ag nanoparticle-loaded nanofibrous mats, a parameter that is crucial for promoting cell proliferation, adhesion, and growth. The synthesis of homogenous, bead-free nanofibers with enhanced diameter was made possible by the addition of silver nanoparticles to the Chitosan PEO polymer solution, making them suitable for drug encapsulation in wound healing applications. The nanofibers also kept a desirable amount of porosity, which increased their capacity for encouraging cell proliferation and tissue regeneration. This study opens up a viable new path for the biomedical engineering industry to create cutting-edge materials.

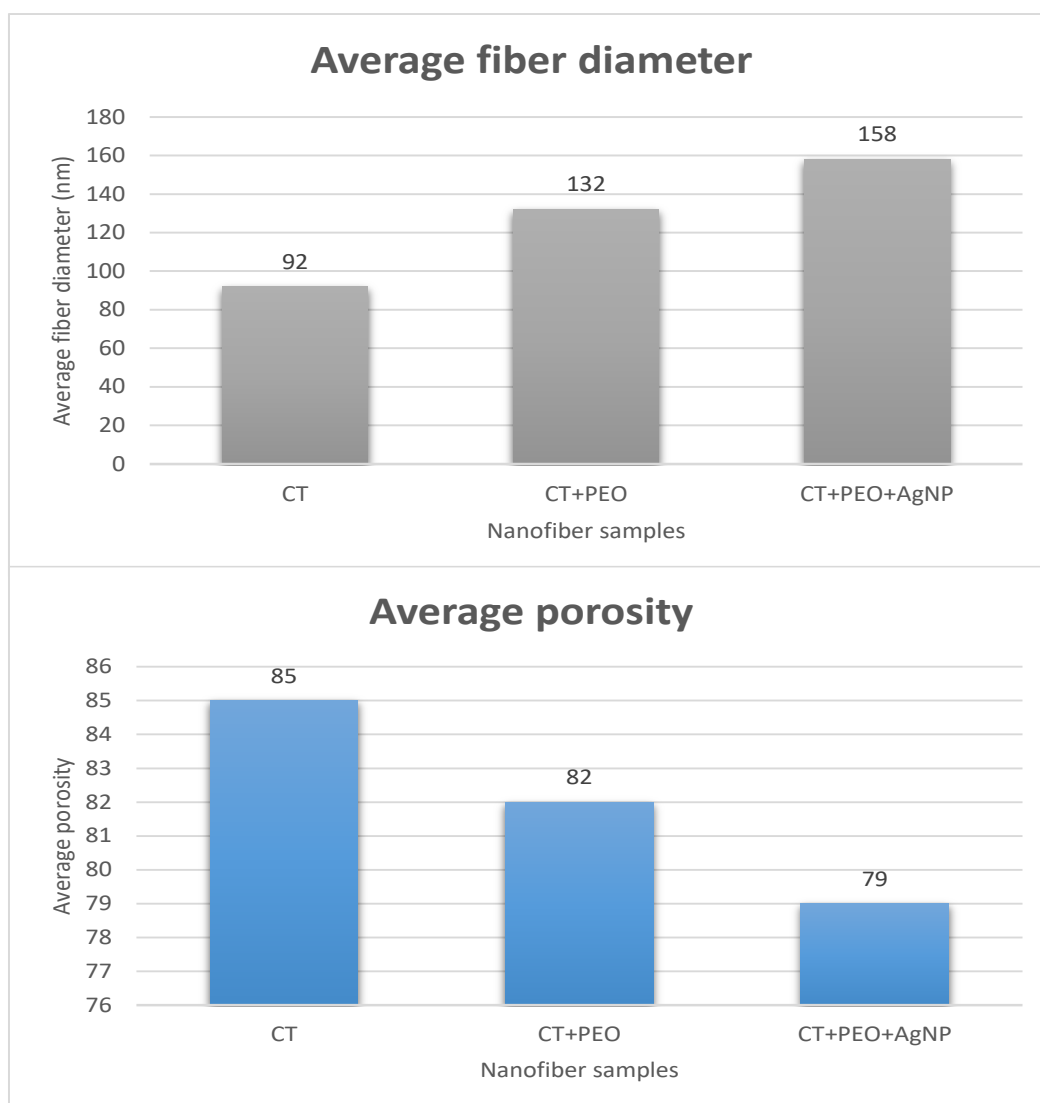


Figure 2: Average fiber diameter and porosity of the samples.

3.3. Characterization

As shown in Figure 3, FTIR analysis was used to look into the unique chemical linkages found inside the manufactured nanofibrous mats. A peak in the spectrum from 3000 to 3400 cm^{-1} in the sample CT + PEO + AgNPs denotes the presence of amide and hydroxylation bonds connected to the functional groups of silver nanoparticles derived from plants. On the other hand, pure chitosan samples often show modest crests in the 3000–3400 cm^{-1} section, which can be attributed to the polysaccharide molecules' intermolecular hydrogen bonds as well as the widening ambiances of their N–H and OH–O bonds. However, because to incomplete interactions with the solution, these peaks were somewhat muted. We did detect N–H and OH/O absorption bands at 3328 cm^{-1} in our experiments. As previously reported by Ridolfi et al. in 2017, samples of CT and CT + PEO also exhibited similar properties, with absorption bands for carbonyl C=O–NHR and amine $-\text{NH}_2$ at 1668 and 1489 cm^{-1} , respectively.

According to Pakravan et al. (2012), the combined solutions of PEO and chitosan with a 50:50 composition displayed peaks corresponding to C–O–C stretching vibrations in the array of 900 to 1200 cm^{-1} , with the highest intensity detected at 1096 cm^{-1} . This is in line with the results of our experiments, where we also found peaks at 1467 cm^{-1} (related to C–H bonding) and 1338 cm^{-1} (connected to the methyl group's C–H distortion). The 900 kDa molecular weight of PEO used in this investigation may have contributed to the OH absorption bands' lack of prominence in our experimental setup.

The FTIR analysis findings indicate the successful electrospinning of the chitosan polysaccharide chains, as evidenced by the occurrence of OH absorption bands at 3400 and 3100 cm^{-1} . This suggests that no components were selectively excluded during the electrospinning process. Further observations from the FTIR analysis include a 3328 cm^{-1} band, indicating H–OH stretching of phenols, C=O widening of ketones and aldehydes (1630 cm^{-1}), a peak at 1378 cm^{-1} equivalent to N=O bending of nitro groups, and bands at 1008 cm^{-1} and 1115 cm^{-1} representing esters' C–O stretching. These bands suggest the formation of interactions between phosphate groups and chitosan amine groups, as reported in earlier studies (Bagheri et al., 2022; Ridolfi et al., 2017; Kargarzadeh et al., 2015).

Additionally, aromatic vibrations of compounds found in the green-synthesized silver nanoparticles were detected at 1450 cm^{-1} , 1500 cm^{-1} , and 1600 cm^{-1} , confirming their presence and indicating the binding of silver ions to chitosan functional groups, consistent with findings by Bagheri et al. in 2022. It's noteworthy that the peaks related to Ag NPs were not prominently visible, likely due to their being masked by the broad and strong bond stretches of the chitosan and PEO matrix. Some irregular small peaks suggest the presence of impurities in the samples.

As mentioned in Martínez-Camacho et al.'s 2013 work, the specimen's biodisponibility is further confirmed by the abundance of NAGA and amino signals, which suggest that these substances have the potential to exert their therapeutic and antimicrobial effects through relations with the cell walls of microorganisms.

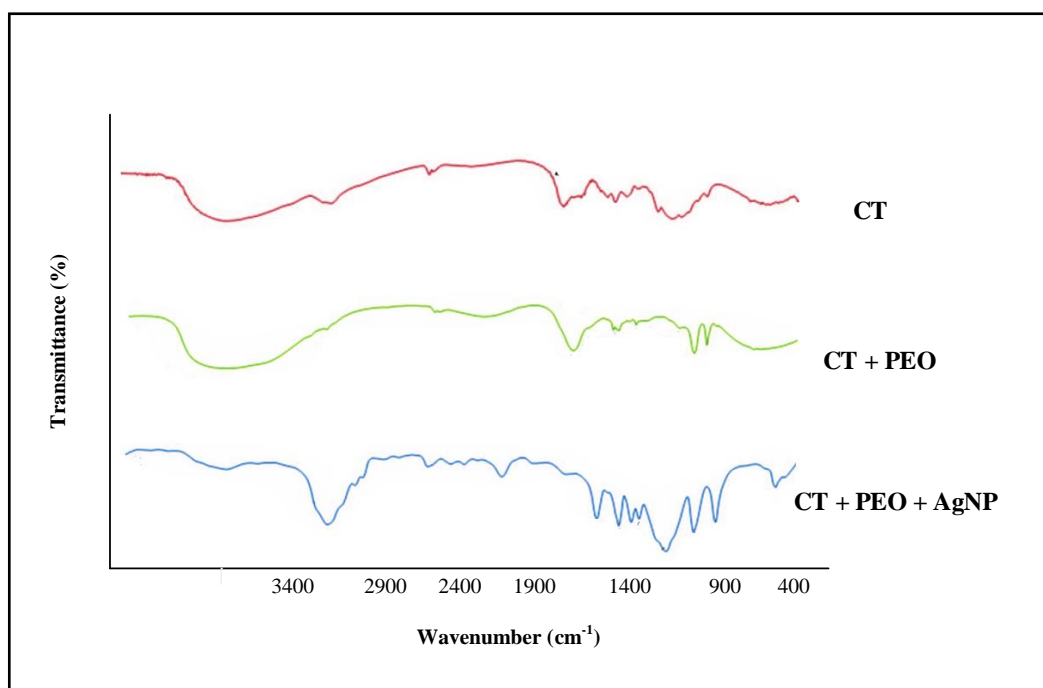


Figure 3: FTIR analysis

3.4. XRD analysis

The composites of CT, PEO, and AgNPs displayed distinctive X-ray diffraction pattern (Figure 4). The crystallinity of chitosan (CT), principally due to its primary chain components, was shown by a noticeable peak at 20° . In addition, peaks at 77.2° , 64.5° , 44.3° , and 38.0° which stand for the (3 1 1), (2 2 0), (2 0 0), and (1 1 1) planes of the cubic design with a face centre of silver nanoparticles (AgNPs), were also noted. These results indicated that the CT + PEO nanofiber matrix included well-dispersed and encapsulated AgNPs (Chen et al., 2019; Ribeiro et al., 2021). These X-ray diffraction results also matched the FTIR study, proving that the composite with 4.0 wt% AgNPs in CT + PEO nanofibers showed a more crystalline phase and a diminished presence of the less crystalline phase. According to Kim's group, the polarisation of the nanofibers caused this preference for the phase, which was brought on by the use of a high DC voltage during the electrospinning procedure (Mandal et al., 2011).

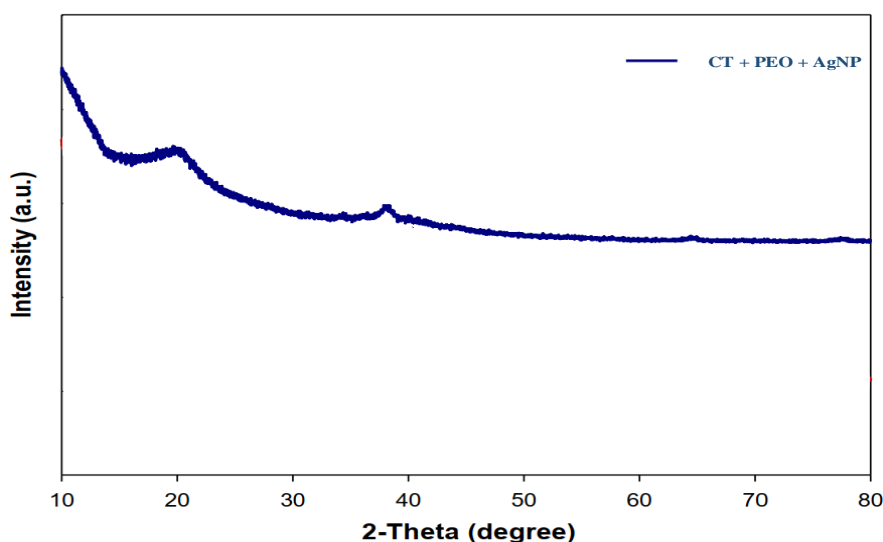


Figure 4: XRD pattern analysis of CT + PEO + AgNP electrospun nanofiber.

3.5. Differential scanning calorimetry analysis

Table 1 shows the nanofibrous mats' peak temperature and thermodynamic values.

Table 1: DSC analysis of the electrospun nanofiber samples.

Nano fiber samples	At melting temperature (T_m)		At glass transition temperature (T_g)	
	T_m ($^{\circ}\text{C}$)	ΔH (J/g)	T_g ($^{\circ}\text{C}$)	ΔH (J/g)
CT	179.78	21.45	62.34	185.12
CT + PEO	185.92	18.91	70.45	162.56
CT + PEO + AgNPs	175.64	19.88	64.92	158.43

Figure 4 displays DSC thermograms of various electrospun nanofibers. The T_m (melting temperature) and T_g (glass transition temperature) of electrospun nanofibers containing Ag NPs (silver nanoparticles) along with CT (Chitosan) and PEO (Polyethylene Oxide) were slightly lower at 64.92°C and 175.64°C, respectively, compared to the pure CT + PEO nanofibers, which had T_m and T_g values of 70.45°C and 185.92°C. This discrepancy can be linked to the electrospun nanofibers' high surface-area-to-volume ratio and the orientation of the polymer chains. The T_m of the CT + PEO nanofibrous mat (185.92°C) increased when Ag NPs were added, as well as the interaction between Chitosan and the PEO matrix was enhanced. In simpler terms, the accumulation of Ag NPs and PEO led to a higher T_m of approximately 185.92°C, and the enthalpy (ΔH) value diminished from 21.45 Jg⁻¹ to 19.88 Jg⁻¹. Nanofibers are potential options for healing wounds because of their porous nature and superior effluent capacity for absorption. Furthermore, they are essential in supporting artery renewal, cell survival and expansion, and infection control due to their capacity to promote oxygen exchange.

4. CONCLUSION

This study looked into the blend electrospinning procedure used to produce synthesized AgNP nanofibers from chitosan/PEO/green for use in wound healing applications. The created nanofibers are beadless, porous, and have a nanoscale structure for maximum biocompatibility. The CT + PEO + AgNP combination of electrospun nanofibers displayed excellent-quality fibers with low bead formation due to the the polymer solution's high surface pressure. The nanoparticle loading in nanofibers is confirmed by the FTIR data. The presence of OH absorption bands in the FTIR study results suggests that the electrospinning of the chitosan polysaccharide chains was successful. With a 150 nm optimum fibre diameter, this effortless, uninterrupted structure is especially well suited for encasing silver nanoparticles for possible uses in the therapy of microbial-infected wound healing. Overall, the findings of this work indicate that recently generated nanofibers with low cytotoxicity, good mechanical qualities, and outstanding biocompatibility may be used as a foundation for wound-healing activities.

DECLARATIONS:

DATA AVAILABILITY STATEMENT

All the data is collected from the simulation reports of the software and tools used by the authors. Authors are working on implementing the same using real world data with appropriate permissions.

FUNDING

No fund received for this project

CONFLICTS OF INTEREST

The authors declare that they have no conflict of interest.

ETHICAL APPROVAL AND HUMAN PARTICIPATION

No ethics approval is required.

REFERENCES

1. Angamma, C.J. and Jayaram, S.H., 2011. Analysis of the effects of solution conductivity on electrospinning process and fiber morphology. *IEEE Transactions on industry applications*, 47(3), pp.1109–1117.
2. Anjum, S., Rahman, F., Pandey, P., Arya, D.K., Alam, M., Rajinikanth, P.S. and Ao, Q., 2022. Electrospun biomimetic nanofibrous scaffolds: a promising prospect for bone tissue engineering and regenerative medicine. *International Journal of Molecular Sciences*, 23(16), p.9206.
3. Antunes, B.P., Moreira, A.F., Gaspar, V.M. and Correia, I.J., 2015. Chitosan/arginine–chitosan polymer blends for assembly of nanofibrous membranes for wound regeneration. *Carbohydrate polymers*, 130, pp.104–112.
4. Bagheri, M., Validi, M., Gholipour, A., Makvandi, P. and Sharifi, E., 2022. Chitosan nanofiber biocomposites for potential wound healing applications: Antioxidant activity with synergic antibacterial effect. *Bioengineering & translational medicine*, 7(1), p.e10254.
5. Bösiger, P., Richard, I.M., Le Gat, L., Michen, B., Schubert, M., Rossi, R.M. and Fortunato, G., 2018. Application of response surface methodology to tailor the surface chemistry of electrospun chitosan–poly (ethylene oxide) fibers. *Carbohydrate polymers*, 186, pp.122–131.
6. Chen, C., Bai, X., Ding, Y. and Lee, I.S., 2019. Electrical stimulation as a novel tool for regulating cell behavior in tissue engineering. *Biomaterials research*, 23, pp.1–12.
7. Chen, Q.J., Zhou, L.L., Zou, J.Q. and Gao, X., 2019. The preparation and characterization of nanocomposite film reinforced by modified cellulose nanocrystals. *International journal of biological macromolecules*, 132, pp.1155–1162.
8. Cui, C., Sun, S., Wu, S., Chen, S., Ma, J. and Zhou, F., 2021. Electrospun chitosan nanofibers for wound healing application. *Engineered Regeneration*, 2, pp.82–90.
9. Elsoud, M.M.A., Elmansy, E.A. and Abdelhamid, S.A., 2022. Economic and Non–Seasonal Source for Production of Chitin and Chitosan. *J. Chem. Rev*, 4(3), pp.222–240.
10. Ganesh, M., Aziz, A.S., Ubaidulla, U., Hemalatha, P., Saravanakumar, A., Ravikumar, R., Peng, M.M., Choi, E.Y. and Jang, H.T., 2016. Sulfanilamide and silver nanoparticles–loaded polyvinyl alcohol–chitosan composite electrospun nanofibers: Synthesis and evaluation on synergism in wound healing. *Journal of Industrial and Engineering Chemistry*, 39, pp.127–135.
11. Geng, X., Kwon, O.H. and Jang, J., 2005. Electrospinning of chitosan dissolved in concentrated acetic acid solution. *Biomaterials*, 26(27), pp.5427–5432.
12. Jirofti, N., Golandi, M., Movaffagh, J., Ahmadi, F.S. and Kalalinia, F., 2021. Improvement of the wound–healing process by curcumin–loaded chitosan/collagen blend electrospun nanofibers: in vitro and in vivo studies. *ACS Biomaterials Science & Engineering*, 7(8), pp.3886–3897.
13. Kargarzadeh, H., Sheltami, R.M., Ahmad, I., Abdullah, I. and Dufresne, A., 2015. Cellulose nanocrystal: A promising toughening agent for unsaturated polyester nanocomposite. *Polymer*, 56, pp.346–357.
14. Khodadoust, M., Mohebbi–Kalhori, D. and Jirofti, N., 2018. Fabrication and characterization of electrospun bi–hybrid PU/PET scaffolds for small–diameter vascular grafts applications. *Cardiovascular engineering and technology*, 9, pp.73–83.

15. Mandal, D., Yoon, S. and Kim, K.J., 2011. Origin of piezoelectricity in an electrospun poly (vinylidene fluoride-trifluoroethylene) nanofiber web-based nanogenerator and nano-pressure sensor. *Macromolecular rapid communications*, 32(11), pp.831–837.
16. Martínez–Camacho, A.P., Cortez–Rocha, M.O., Graciano–Verdugo, A.Z., Rodríguez–Félix, F., Castillo–Ortega, M.M., Burgos–Hernández, A., Ezquerra–Brauer, J.M. and Plascencia–Jatomea, M., 2013. Extruded films of blended chitosan, low density polyethylene and ethylene acrylic acid. *Carbohydrate polymers*, 91(2), pp.666–674.
17. Mirhaj, M., Labbaf, S., Tavakoli, M. and Seifalian, A.M., 2022. Emerging treatment strategies in wound care. *International Wound Journal*, 19(7), pp.1934–1954.
18. Pakravan, M., Heuzey, M.C. and Ajji, A., 2012. Core-shell structured PEO–chitosan nanofibers by coaxial electrospinning. *Biomacromolecules*, 13(2), pp.412–421.
19. Pourshahrestani, S., Zeimaran, E., Kadri, N.A., Mutlu, N. and Boccaccini, A.R., 2020. Polymeric hydrogel systems as emerging biomaterial platforms to enable hemostasis and wound healing. *Advanced healthcare materials*, 9(20), p.2000905.
20. Puri, A., Sahai, N., Ahmed, T. and Saxena, K., 2023. 3D bioprinting for diagnostic and therapeutic application. *Materials Today: Proceedings*.
21. Ribeiro, A.S., Costa, S.M., Ferreira, D.P., Calhelha, R.C., Barros, L., Stojković, D., Soković, M., Ferreira, I.C. and Figueiro, R., 2021. Chitosan/nanocellulose electrospun fibers with enhanced antibacterial and antifungal activity for wound dressing applications. *Reactive and Functional Polymers*, 159, p.104808.
22. Ridolfi, D.M., Lemes, A.P., de Oliveira, S., Justo, G.Z., Palladino, M.V. and Durán, N., 2017. Electrospun poly (ethylene oxide)/chitosan nanofibers with cellulose nanocrystals as support for cell culture of 3T3 fibroblasts. *Cellulose*, 24, pp.3353–3365.
23. Sahai, N., Gogoi, M. and Tewari, R.P., 2021. 3D printed chitosan composite scaffold for chondrocytes differentiation. *Current medical imaging*, 17(7), pp.832–842.
24. Shahid, M.A., Ali, A., Uddin, M.N., Miah, S., Islam, S.M., Mohebbullah, M. and Jamal, M.S.I., 2021. Antibacterial wound dressing electrospun nanofibrous material from polyvinyl alcohol, honey and Curcumin longa extract. *Journal of Industrial Textiles*, 51(3), pp.455–469.
25. Shi, D., Wang, F., Lan, T., Zhang, Y. and Shao, Z., 2016. Convenient fabrication of carboxymethyl cellulose electrospun nanofibers functionalized with silver nanoparticles. *Cellulose*, 23, pp.1899–1909.
26. Srivastava, C.M., Purwar, R. and Gupta, A.P., 2019. Enhanced potential of biomimetic, silver nanoparticles functionalized *Antheraea mylitta* (tasar) silk fibroin nanofibrous mats for skin tissue engineering. *International journal of biological macromolecules*, 130, pp.437–453.
27. Stoica, A.E., Chircov, C. and Grumezescu, A.M., 2020. Nanomaterials for wound dressings: an up-to-date overview. *Molecules*, 25(11), p.2699.
28. Tan, L., Zhou, Z., Liu, X., Li, J., Zheng, Y., Cui, Z., Yang, X., Liang, Y., Li, Z., Feng, X. and Zhu, S., 2020. Overcoming multidrug-resistant MRSA using conventional aminoglycoside antibiotics. *Advanced Science*, 7(9), p.1902070.
29. Vandghanooni, S. and Eskandani, M., 2019. Electrically conductive biomaterials based on natural polysaccharides: Challenges and applications in tissue engineering. *International journal of biological macromolecules*, 141, pp.636–662.